Marine Pollution Bulletin 222 (2026) 118787

Contents lists available at ScienceDirect

Marine Pollution Bulletin

journal homepage: www.elsevier.com/locate/marpolbul

The response of phytoplankton to pH-equilibrated ocean alkalinization: A mesocosm experiment with harbour waters

Sara Groppelli [a,*], Davide Calvi [a], Federico Comazzi [b], Samira Jamali Alamooti [d], Arianna Azzellino [c], Eleonora Barbaccia [c], Sarah Caronni [a], Piero Macchi [d], Guido Raos [d], Daniela Basso [a]

[a] Department of Earth and Environmental Sciences (DISAT), University of Milano-Bicocca, Piazza della Scienza, 20126, Milano, Italy
[b] Limenet s.r.l., 23851, Galbiate, LC, Italy
[c] Civil and Environmental Engineering Department (DICA), Politecnico di Milano, Piazza Leonardo da Vinci 32, 20133, Milano, Italy
[d] Department of Chemistry, Materials and Chemical Engineering "Giulio Natta", Politecnico di Milano, Via Luigi Mancinelli 7, 20131, Milano, Italy

ARTICLE INFO

Keywords:
Carbon dioxide removal (CDR)
Bicarbonate-enriched seawater
Diatoms
Dinoflagellates
Silicon uptake
Limenet® technology

ABSTRACT

Mitigating global warming requires urgent reductions in carbon dioxide (CO_2) emissions and the development of Carbon Dioxide Removal (CDR) strategies. pH-equilibrated Ocean Alkalinization ($pH_{eq}OA$) has emerged as a promising method to enhance CO_2 sequestration while minimizing potential environmental risks. This study investigates the ecological impact of $pH_{eq}OA$ on phytoplankton communities through a mesocosm experiment in the Gulf of La Spezia (Italy) using local seawater treated with Limenet® technology. We assessed planktonic responses to different levels of bicarbonate-enriched seawater (Control, Low, Medium, High, Oversaturated) by monitoring changes in carbonate chemistry, nutrient availability, and phytoplankton community composition over 15 days. Results revealed that $pH_{eq}OA$ treatments (excluding the oversaturated condition) helped maintain greater ecological stability, reducing the rate of diatom/dinoflagellate community shifts and supporting higher silicon uptake, particularly by diatoms. In contrast, oversaturation led to carbonate precipitation and a significant loss of added alkalinity. The findings suggest that moderate $pH_{eq}OA$ may enhance phytoplankton resilience and promote diatom activity under altered carbonate chemistry. This study underscores the need for further research to evaluate the broader ecological implications of $pH_{eq}OA$.

1. Introduction

Achieving the goal of keeping global warming below 2°C requires urgent and significant cuts in emissions. Additionally, it will be necessary to implement various Carbon Dioxide Removal (CDR) strategies capable of extracting hundreds of gigatons of CO_2 from the atmosphere and storing it safely in long-term carbon reservoirs for thousands of years (Rogelj et al., 2018; Intergovernmental Panel on Climate Change (IPCC), 2022). However, only a few CDR methods have the potential to create a significant impact at the global scale, and all of them are associated with potential environmental implications for the Earth system (Fuss et al., 2018). The Accelerated Weathering of Limestone (AWL) method involves reacting CO_2 with seawater and calcium carbonate ($CaCO_3$) to produce bicarbonates (HCO_3^-), which are then discharged into the ocean (Rau and Caldeira, 1999; Caldeira and Rau, 2000). A critical challenge in AWL processes is preventing the return of CO_2 into the atmosphere through precipitation of carbonate minerals like aragonite and calcite. This reaction, triggered by supersaturation, would undermine storage efforts (Suitner et al., 2024; Riebesell et al., 2023). Although the field is still in its early stages, several scientific papers have begun to lay the groundwork for understanding the effects of Ocean Alkalinity Enhancement. Among the most relevant studies are those which have analyzed both physicochemical aspects—like carbon storage capacity and changes in seawater pH—and possible biological impacts on microorganisms and marine communities (Bach et al., 2019). Other works, such as this by Renforth (2012) (Kruger and Renforth, 2012), have focused on broader environmental implications and the uncertainties related to large-scale deployment scenarios.

---

* Corresponding author.
E-mail addresses: s.groppelli1@campus.unimib.it (S. Groppelli), d.calvi2@campus.unimib.it (D. Calvi), federico.comazzi@limenet.tech (F. Comazzi), samira.jamali@polimi.it (S.J. Alamooti), arianna.azzellino@polimi.it (A. Azzellino), eleonora.barbaccia@polimi.it (E. Barbaccia), sarah.caronni@unimib.it (S. Caronni), piero.macchi@polimi.it (P. Macchi), guido.raos@polimi.it (G. Raos), daniela.basso@unimib.it (D. Basso).

https://doi.org/10.1016/j.marpolbul.2025.118787
Received 11 July 2025; Received in revised form 27 August 2025; Accepted 26 September 2025

Studies also highlight risks associated with pH spikes and chemical imbalances from ocean liming, emphasizing the importance of pH-equilibrated solutions to minimize unpredictability and harmful reactions (Iglesias-Rodríguez et al., 2023). A further enhancement, Buffered Accelerated Weathering of Limestone (BAWL) uses excess CO_2 and calcium hydroxide ($Ca(OH)_2$ = slaked lime) to create a pH-equilibrated bicarbonate solution (Caserini et al., 2021; De Marco et al., 2023). This method, investigated for its technical and economic feasibility, has led to the development of the Limenet® process (Limenet®, 2024). Limenet® directly combines CO_2 with $Ca(OH)_2$ and seawater in reactors, yielding a bicarbonate-enriched solution with natural seawater pH and high alkalinity, which helps counter ocean acidification while minimizing the risks of CO_2 re-release (Varliero et al., 2024). Limenet® method represents a pH-equilibrated ocean alkalinization ($pH_{eq}OA$), in which renewable energy is used to mitigate emissions associated with slaked lime production, enhancing the overall efficiency of the process. Additionally, the sustainability of this method is assessed through methodologies such as the Life Cycle Assessment (LCA). LCA studies provide a comprehensive evaluation of the environmental impacts, such as CO_2 emissions, considering the energy consumption and the resources used throughout the entire process (Terlouw et al., 2021). These assessments emphasize the importance of renewable energy integration and optimized material use to maximize the net carbon sequestration potential and reduce overall environmental impacts (Foteinis et al., 2022). Recent pilot experiments tested the stability of bicarbonate-enriched seawater created by the Limenet® process. Natural seawater treated and monitored over three months showed stable CO_2 preservation up to a carbon addition of 1500 μmol/L, equivalent to a total Dissolved Inorganic Carbon (DIC) of about 3800 μmol/L. At higher concentrations (e.g., carbon additions of 1800 μmol/L), carbonate precipitation and efficiency loss were observed. Similarly, artificial seawater treated with solid sodium bicarbonate exhibited carbonate precipitation for DIC increases above 1200 μmol/L (Varliero et al., 2024).

Changes in carbonate chemistry from $pH_{eq}OA$ may affect plankton communities, which are vital to ocean food webs and the carbon cycle. At current CO_2 levels, phytoplankton use energy-demanding CO_2 Concentrating Mechanisms (CCM) due to low carbon uptake efficiency (Raven et al., 2011; Hopkinson, 2014; Spreitzer and Salvucci, 2002).

These microorganisms adjust physiological processes, such as energy use and nutrient allocation, to optimize carbon uptake under varying growth conditions. Consequently, shifts in carbonate chemistry induced by $pH_{eq}OA$ may enhance photosynthesis (due to increased HCO_3^- availability) and/or benefit calcifying organisms (via higher pH and improved calcium carbonate saturation) (Bach et al., 2013). However, species-specific differences in the ability to take up carbon and in carbon acquisition efficiency suggest that sensitivity to $pH_{eq}OA$ could vary among phytoplankton, potentially leading to diverse effects on their fitness and, consequently, altering community composition and biodiversity (Xin et al., 2024). Additionally, microzooplankton, which consume primary producers, may be indirectly affected by changes in prey availability or directly influenced by pH-related physiological impacts (Camatti et al., 2024). These changes could cascade through trophic levels (Pedersen and Hansen, 2003), influencing higher organisms and microbial loops (Calbet, 2008). Phytoplankton and microzooplankton exhibit a high tolerance under equilibrated Ocean Alkalinity Enhancement (OAE) conditions in the oligotrophic ocean (Xin et al., 2024; Traboni et al., in press). Furthermore, Sanchez et al. (Sánchez et al., 2024) found the equilibrated approach as a safe use of OAE in oligotrophic plankton food webs, showing food web resistance and zooplankton tolerance to moderate CO_2-equilibrated chemical perturbations. Moreover, an uncontrolled potential boost to calcifiers might result in an additional CO_2 source, thus reducing the efficiency of the $pH_{eq}OA$. The potential impacts of $pH_{eq}OA$ on the health of planktonic organisms, species diversity, size distribution within plankton communities, energy transfer in food webs, and global carbon cycle dynamics remain largely uncertain (Sánchez et al., 2024; Marañón, 2015; Moreno et al., 2022).

While it may seem intuitive to use findings from ocean acidification studies to predict the effects of $pH_{eq}OA$ - given that these processes alter carbonate chemistry in opposite directions - this approach is overly simplistic. The ecological consequences of $pH_{eq}OA$ may not directly mirror the inverse effects of ocean acidification, as the responses of marine ecosystems could be asymmetrical (Bach et al., 2013; Zickfeld et al., 2021). This is particularly relevant in the case of pH-equilibrated technology, where no direct alteration of seawater pH occurs. The current literature highlights the need for more in situ experiments and predictive models to fill existing knowledge gaps. In particular, there is a call for integrated studies that involve different disciplines and consider both climate benefits and potential risks to marine biodiversity and coastal communities. Therefore, it is crucial to conduct targeted research to thoroughly investigate the ecological implications of $pH_{eq}OA$ before advancing its broader application. A deeper understanding of how $pH_{eq}OA$ influences plankton ecosystems is essential to determine the feasibility and potential scalability of this negative emissions technology (NET) (IPCC, 2014; National Academies of Sciences, Engineering, and Medicine, 2019).

This study presents results from an in situ mesocosm experiment on $pH_{eq}OA$ based on the Limenet® technology, assessing its environmental impact and potential benefits for phytoplankton in Italy's Gulf of La Spezia.

2. Materials and methods

2.1. Study site and experimental design

The Ligurian Sea hosts a dynamic and diverse phytoplankton community that varies seasonally and spatially in response to environmental conditions, such as nutrient availability, water column stratification, and mesoscale physical processes (Mayot et al., 2020). This community is composed of different size classes, including microphytoplankton and nanophytoplankton, each playing a crucial role in the marine ecosystem. Microphytoplankton, primarily represented by diatoms and dinoflagellates, thrive under nutrient-rich conditions. Diatoms dominate bloom events in winter and in spring, while dinoflagellates can exhibit mixotrophic behaviours and form harmful algal blooms (HABs) especially in late summer. Nanophytoplankton, particularly coccolithophores like *Emiliania huxleyi*, become more prominent during stratified summer conditions, contributing to the biological carbon pump. Seasonal dynamics influence phytoplankton abundance, with winter deep convection leading to low biomass, followed by spring diatom blooms, summer stratification favoring smaller phytoplankton, and autumn mixing triggering secondary bloom events (Mayot et al., 2020). The Gulf of La Spezia presents a complex hydrographic system influenced by seasonal variations, freshwater inputs, and anthropogenic activities. Water temperature ranges from 12 - 14 °C in winter to 22–26 °C in summer, reflecting the impact of solar radiation and local currents. Conductivity typically ranges from 50 to 55 mS cm^{-1}, though it may decrease near coastal areas due to freshwater discharge. The pH values typically range between 7.8 and 8.2, indicating a slightly alkaline marine environment. Dissolved oxygen (DO) fluctuates between 80 % and 100 % saturation, though localized reductions may occur in poorly ventilated areas with high organic loads. Nutrient levels vary significantly across the gulf, with nitrate (NO_3^-) concentrations between 1 and 5 μM, nitrite (NO_2^-) generally below 1 μM, and phosphate (PO_4^{3-}) ranging from 0.1 to 0.5 μM. BSi (SiO_2) levels fluctuate from 1 to 10 μM, often peaking near riverine inputs (Ciuffardi et al., 1973).

Mesocosms are sophisticated experimental tools that bridge field and laboratory techniques, allowing researchers to control specific environmental parameters while creating realistic exposure scenarios that closely mimic natural conditions (Riebesell et al., 2023; Alexander et al., 2016).

The mesocosm experiment was conducted at Porto Mirabello (44°06′04.7"N, 9°49′40.6″E) in La Spezia (Italy), using fifteen land-based mesocosms, with a capacity of 1000 L each, built with transparent Low-Density PolyEthylene (LDPE) bags. Each mesocosm was precisely filled on 14 March 2024 with a submersible pump equipped with a flow meter, by diluting natural seawater with five different percentages of bicarbonate-rich seawater. A pilot-scale Limenet® system, with a Technology Readiness Level (TRL) of 6 for the Limenet® storage process was used, capable of treating 1 kg h^{-1} of CO_2. The five treatments, from the "not treated" (Control) to the most extreme treatment level (Oversaturated), are characterized by an increase in the alkalinity and aragonite saturation level (Table 1). The volume of the Limenet® bicarbonate-rich seawater and the concentrations of added TA are reported in Table 1, along with the aragonite saturation state (Ω_{arag}), calculated using the CO2SYS Excel Macro (version 2.5) (Pierrot et al., 2006) based on the characteristics of the seawater collected in La Spezia. The calculations utilized carbonate system constants from Mehrbach et al. (Mehrbach et al., 1973) refit by Dickson & Milleo (Dickson and Millero, 1987) with supplementary constants from Dickson (Dickson, 1990) for $KHSO_4$, and from Uppström (Uppström, 1974) for total borate concentration. Treatments were replicated three times.

Ω_{arag} is a critical indicator of the potential for carbonate mineral precipitation. It is defined as the ratio of the molar concentrations of Ca^{2+} and CO_3^{2-} ions to the stoichiometric solubility product of aragonite in seawater (Zeebe and Wolf-Gladrow, 2001). According to Moras et al. (Moras et al., 2022), a safe threshold for Ω_{arag} is approximately 5, beyond which runaway precipitation and CO_2 degassing may occur. In this experiment, the OS treatment represented oversaturated seawater, specifically designed to investigate the potential adverse effects of operating above this threshold.

Mesocosms were coded as shown in Fig. 1, where P stands for pool.

The mesocosms were randomly arranged within a transparent cover to minimize external environmental influences. Each group of three mesocosms was surrounded by a containment pool filled with water, which acted as a buffer against temperature fluctuations (Fig. 1). To maintain stable conditions for the planktonic organisms inside the mesocosms, the water in the pools was replaced daily, preventing overheating. The experiment spanned 15 days, with samples collected every two days.

2.2. Environmental monitoring and alkalinity control

Throughout the experiment, temperature, pH, conductivity, and dissolved oxygen were monitored three times per day using a Revio Giorgio Bormac multiparametric probe. The pH sensor operates with an accuracy of ±0.02 pH and is calibrated at three points (4.01, 7.00, and 10.01), covering a measurement range from 0 to 14 pH. The conductivity sensor ensures an accuracy of ±2 % full scale (f.s.) and supports two-point calibration at 1413 μS and 12.88 mS. For dissolved oxygen measurement, the probe provides an ORP resolution of 1 mV and a measurement range of −1000 to +1900 mV ORP, with single-point calibration at 100 % saturation. The multiparametric probe was calibrated before each analysis, to ensure consistency across treatments. Another important chemical parameter that required special attention was alkalinity, which was measured on site immediately after plankton sampling, every two days, using an automatic alkalinity titrator (Hanna Instruments HI84531 mini titrator with a combined pH meter and thermometer, low titrant range, range 30.0–400.0 mg L^{-1} $CaCO_3$, accuracy: ± 1 mg L^{-1}) with an acid pump and electrode. Both the acid pump and the electrode were calibrated before each analysis. The electrode was calibrated using buffer solutions with pH values of 4.01, 7.01, and 8.30 to ensure accuracy. The acid pump was calibrated by preparing a sample with a stirrer inside it, using a clean tip and a 2000 μL automatic pipette to precisely add 4 mL of Calibration Standard into a clean beaker. The beaker was then filled up to the 50 mL mark with distilled or deionized water. The total alkalinity (TA) of natural seawater was measured and designated as the TA of the control (TA_C), serving as the baseline. The TA values of other treatments (TA_T), which were higher than the control in proportion to the added $Ca(OH)_2$ concentrations, were measured and compared against TA_C. This comparison is represented as TA_T - TA_C.

Table 1
Volume of treated seawater over the total 1000 L volume, Total Alkalinity (TA) concentrations and the aragonite saturation state (Ω_{arag}) for the 5 different treatments. C = control; L = low; M = medium; H = high; OS = Oversaturated.

Treatment	Treated volume (L - %)	TA addition (μeq L^{-1})	Ω_{arag}
C	0–0	0	3.4
L	33–3.3 %	262	3.9
M	67–6.7 %	524	4.3
H	133–13.3 %	1048	5.2
OS	263–26.3 %	2096	7.1

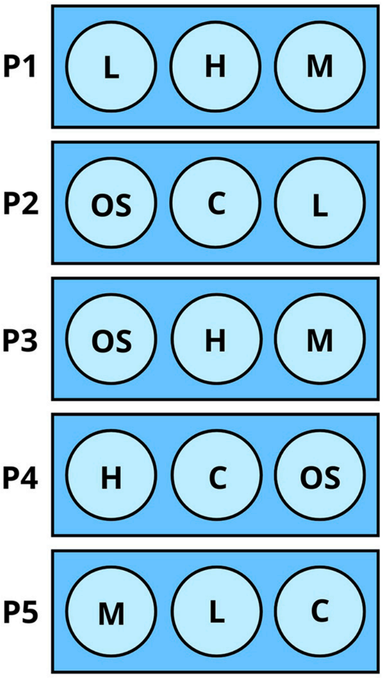

Fig. 1. Scheme of the experimental design. Control (C): P2C, P4C, P5C. Low (L): P1L, P2L, P5L. Medium (M): P1M, P3M, P5M. High (H): P1H, P3H, P4H. Oversaturated (OS): P2OS, P3OS, P4OS.

2.3. Nutrient analysis

The concentrations of nutrients in the mesocosms, essential for phytoplankton growth and sustenance, was measured on a regular basis. Ammonium and phosphates were measured every two days in all of the 15 mesocosms. TSi was measured in each mesocosm at the beginning of the experiment, and then in mesocosms P1L, P2C, P3M, P4H, P3OS every 4 and then 2 days, in order to monitor the expected depletion due to biological uptake in the enclosures. Water samples from each mesocosm were sent for nutrient analyses to the Ecology laboratory of the University of Milano-Bicocca (UNIMIB). No additional nutrients were introduced during the 15-days experiment in order to avoid unnecessary variables due to further manipulation of the experimental setting. The determination of ammoniacal nitrogen (NH_4^+) was performed by removing chloride interference using the Hach LCW 925 kit, containing silver oxide (Ag_2O) to precipitate silver chloride (AgCl). NH_4^+ concentration was measured colorimetrically with the Hach LCK 304 kit (range: 0.015–2.0 mg L^{-1} NH_4^+-N), recording absorbance at 655 nm after a 15-min reaction. Orthophosphate analysis followed the protocol outlined in the Monitoring Program for Marine and Coastal Environment Control (Cicero and Di Girolamo, 2001). For Total silicon (TSi) analysis, samples were diluted 1:10 with Milli-Q water and acidified to 2 % nitric acid (1:1.03 dilution); An ICP-OES (Optima 7000 DV, PerkinElmer) with WinLab32 software was used, with calibration curves built from three standard levels. Reagents included 65 % nitric acid (Sigma Aldrich), Milli-Q water, and 1000 mg L^{-1} standard Si (2 % HNO_3, PerkinElmer), with calibration solution prepared in 2 % HNO_3. Results, processed via calibration curves, showed detection limits of 0.02 mg L^{-1} for TSi, with values below these limits noted as *nd*. Silicon uptake was determined under different experimental conditions to better understand its dynamics and implications for diatom growth. In agreement with Exley & Sjöberg (Exley and Sjöberg, 2014) we assumed that the uncharged species $Si(OH)_4$ is predominating under normal seawater conditions. Given the different experimental conditions (C, L, M, H, and OS bicarbonate conditions), each with varying initial TSi concentrations, analyses were performed at two time points: day 1 and day 5 for each treatment. Using the molecular weight of $Si(OH)_4$ (96.1 g mol^{-1}), concentrations were converted from ppm to μmol/L and DSi uptake ($\Delta Si(OH)_4$) was calculated as the difference in $Si(OH)_4$ concentration between day 1 and day 5 for each treatment.

2.4. Plankton sampling and analysis

The characteristics of the seawater in the La Spezia harbour inherently limit the presence of planktonic calcifying organisms, such as coccolithophores, which are typically associated with open water ecosystems and display reduced diversity in coastal regions (Baumann et al., 2005), while a microphytoplankton community dominated by silicifying organisms was expected.

For microphytoplankton analysis, 1 L of water was collected from each mesocosm and immediately preserved with 1 % Lugol's solution, following the method described by Zingone et al. (Zingone et al., 2010). Cell abundance was determined using an inverted microscope (EUROMEX FE 2935) equipped with a sedimentation chamber (26 mm diameter, 5 mL volume). Samples were left to settle for approximately 6 h before analysis. Cells were counted along four perpendicular transects within each sedimentation chamber, allowing for efficient sub-sampling while minimizing bias from uneven cell distribution (Zingone et al., 2010). All cells along each transect were counted and identified at the genus level for diatoms (Avancini et al., 2006), and at the lowest possible suprageneric level for the other components. The phytoplankton concentration was calculated with the formula (Zingone et al., 2010):

$$C = N \text{ x factor x } 1000/v$$

where:

C = phytoplanktonic concentration expressed as cells L^{-1};
N = number of cells counted;
v = sedimented sample volume (mL);
factor = ratio of total chamber area to explored area (π × r /2 n h);
r = radius of the sedimentation chamber (mm);
h = side of the grid or diameter of the field of view (mm);
n = number of observed transects.

We calculated the Shannon diversity index (H′) (Shannon, 1948) exclusively on the diatom association, which was the dominant component in all samples.

2.5. Silicon uptake

Silicon uptake was estimated (Kristiansen and Hoell, 2002) from the decrease in Si concentration, converted from ppm to μmol L^{-1} using the molecular weight of SiO_2. Volumetric uptake rates (μmol m^{-3} h^{-1}) were calculated as ΔSi/Δt, where ΔSi is the change in dissolved Si concentration and Δt is time in hours. Cell-specific uptake (ng Si $cell^{-1}$ h^{-1}) was obtained by normalizing to diatom abundance (N, cells L^{-1}), according to the relation:

$$U_c = \Delta Si \text{ x } M_{Si}/N \text{ x } \Delta t$$

Where M_{Si} is the atomic mass of silicon (ng μmol^{-1}).

2.6. Statistical analysis

The temporal variability of the phytoplankton community was investigated by analysing the log-transformed ratio (base 10) between diatoms and dinoflagellates abundances among days and treatments. A Generalised Linear Model (hereinafter called GLM) (Rutherford, 2001) was used of the kind:

$$y_{ijk} = \mu + \alpha_i + \beta_j + \alpha\beta_{ij} + \varepsilon_{ijk}$$

where:

y_{ijk}: k_{th} log transformed ratio of diatoms/dinoflagellates of the i_{th} treatment and the j_{th} day;
μ: true overall mean;
α_i: incremental effect of treatment i (Factor A);
β_j: incremental effect of day j of experiment, (Factor B);
$\alpha\beta_{ij}$: treatment*day interaction term;
ε_{ijk}: error for the k_{th} observation of the i_{th} level of the treatment and of the j_{th} day.

GLM has been used to test the effect of the treatments and of the experiment duration (i.e. days).

A second GLM assessed diatom diversity by day and treatment:

$$y_{ijk} = \mu + x_i + \alpha_i + \varepsilon_{ijk}$$

where:

y_{ijk}: k_{th} log transformed ratio of diatoms/dinoflagellates of the i_{th} treatment and the j_{th} day;
μ: true overall mean;
x_j: incremental effect of day i of experiment, (covariate);
α_j: incremental effect of treatment j (Factor A);
ε_{ijk}: error for the k_{th} observation of the i_{th} level of the treatment and of the j_{th} day.

Finally, A One-way ANOVA was instead used to contrast diatoms and dinoflagellates abundance across treatments at day 1.

3. Results

3.1. Abiotic parameters

Temperature (Fig. 2A) trends remain consistent across all experimental conditions (C, L, M, H, and OS). The recorded values range between 15 °C and 20 °C, showing only minor daily fluctuations and no significant differences among the groups.

Dissolved oxygen levels, expressed as a percentage, exhibit minor variability among the treatments (Fig. 2B). Across all experimental groups, values fluctuate between 80 % and 100 %, with no distinct trends differentiating the five conditions significantly. While minor daily fluctuations are detectable, overall, oxygen levels remain relatively stable throughout the study.

Conductivity values (Fig. 2C) fluctuate within a narrow range, between 49.3 and 51.5 mS cm^{-1}, corresponding to a salinity of 32.3–33.8 ‰. Condition C exhibits the lowest overall fluctuation, maintaining a

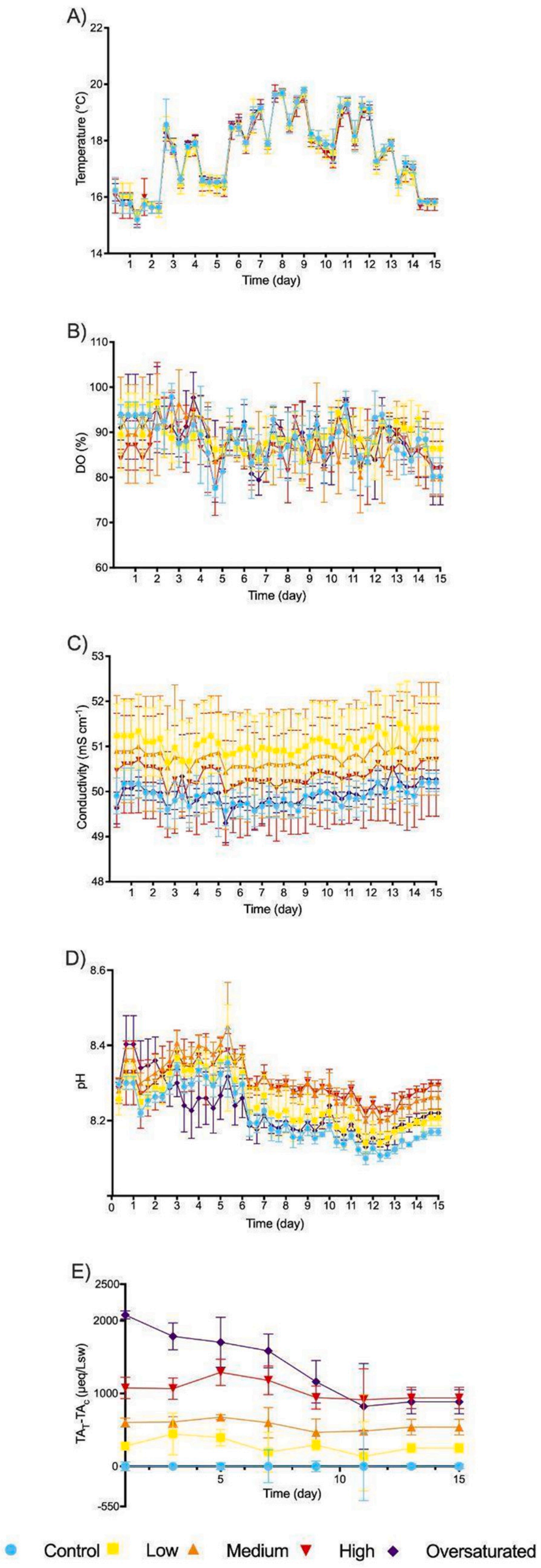

Fig. 2. Temporal variations of key environmental parameters over 15 days under the different alkalinization treatments. A) Temperature (°C); B) Dissolved oxygen (% saturation); C) Conductivity (mS cm^{-1}); D) pH; E) Total alkalinity differences between treated and control mesocosms (TA_T - TA_C).

stable trend around 50 mS cm^{-1}. Condition L shows higher conductivity levels compared to the control, with slight variability over time. Condition M follows a similar trend to L but with consistently higher conductivity values. Condition H displays the highest overall conductivity, remaining close to 51.5 mS cm^{-1}. Conversely, condition OS fluctuates below the other treatments and stays close to 49 mS cm^{-1} for most of the experiment. Regarding pH variations (Fig. 2D), C exhibits the lowest pH levels throughout the study, gradually decreasing to approximately 8.1 before stabilizing. Condition L starts with higher initial pH values compared to the control, then shows a downward trend around day 5, followed by a slight increase toward the end of the experiment. Similarly, condition M follows the same pattern as L, with initially higher pH values that decline between days 5 and 10, before experiencing a modest recovery. Condition H maintains the highest pH levels overall, consistently staying above 8.2 and showing a slight increase at the end of the study. Condition OS begins with pH values similar to M but experiences a sharper decrease around day 5 and remains lower for the duration of the experiment.

The increase in alkalinity along with a rebalancing of pH (close to pH of natural seawater) reveals that the treated seawater was effectively storing CO_2 in the form of bicarbonates. Due to runaway calcium carbonate precipitation, the OS treatment underwent a noticeable loss of alkalinity immediately after the mesocosm preparation. This was revealed by a 57 % decrease in added TA compared to the control treatment after 15 days. In contrast, the reductions for the H, M, and L treatments were approximately 12 %, 10 %, and 10 %, respectively (Fig. 2E).

Nutrient concentration decreases over time. TSi (Fig. 3A) shows a slower decrease in C than in the other treatments. At day 1, all conditions start with relatively high TSi concentrations, with the H group showing the highest initial TSi concentration. Over time, a consistent decrease in TSi concentration is observed across all conditions. By day 9, TSi levels in all treatments drop below detection limits until the end of the experiment.

Conversely, for P-PO_4 (Fig. 3B) and N-NH_4 (Fig. 3C), no statistically significant differences were observed among the treatments, with values around 5,4 µg L^{-1} and 78,7 µg L^{-1} respectively, indicating similar behavior across the experimental conditions for these nutrients.

3.2. *Phytoplankton response*

The analyses revealed that the plankton community was overall dominated by diatoms, with species from the genus *Chaetoceros* consistently representing the most abundant and widespread group across all treatments and sampling times. Moreover, no major morphological changes of *Chaetoceros* were observed during the first five days of the experiment; the cells remained in chain colonies and the setae were attached. However, diatom dominance was declining in the course of the experiment, making way for dinoflagellates, which showed a notable increase starting from day 5 (Fig. 4). The initial conditions across treatment levels showed a slight inconsistency, due to apparent higher diatom abundances compared to controls, although not statistically significant. To facilitate a clearer comparison, the log-transformed diatom/dinoflagellate ratio was employed as an indicator. The rate of decline of this ratio was then used to assess changes in community composition more effectively.

The rate of decline of the diatom/dinoflagellate ratio over time was used as an indicator of the degree of alteration within each treatment. A steeper slope, indicating a quicker decline, reflected larger and more rapid changes in the ratio, indicating significant ecological shifts in the balance between the two phytoplankton groups. Conversely, a gentler slope, indicating a slower decline, suggested slower rates of change or less pronounced shifts, pointing to a more stable or minimally impacted ratio over the observation period.

The temporal dynamics of diatoms and dinoflagellates under the five experimental treatments highlights distinct patterns in abundance over

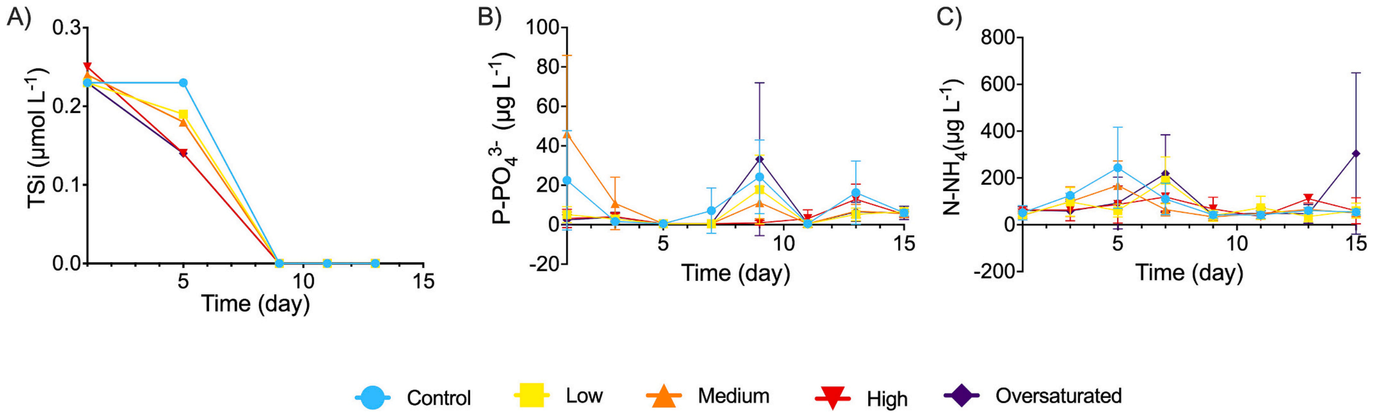

Fig. 3. Temporal variations of nutrient concentrations. A) Total Silicon; B) P-PO_4^{3-}; C) N-NH_4.

time and consistently show one order of magnitude higher abundance of diatoms vs. dinoflagellates across all treatments. Diatoms maintained population sizes in the range of 10^6 individuals, dominating the community in terms of cell abundance, whereas dinoflagellates remained at lower levels, in the 10^5 range.

Diatom abundance generally has decreased throughout the experiment, particularly in the C and OS treatments, where a sharp decline was observed after the initial days. In contrast, under the L, M and H treatments, diatom populations exhibit greater stability. Dinoflagellates, on the other hand, displayed an opposite trend, markedly increasing in number over time.

Diatom diversity (Fig. 5), measured by the Shannon index (H′), exhibited a general decline across all treatments during the experiment (P-value <0.001, see Table 2). At the beginning, the Shannon index was relatively high for all treatments. Diatom diversity declined over time in all treatments ($P < 0.001$; Table 2). Control and Low treatments showed the fastest decline ($P \leq 0.001$; Table 3), while M and H treatments did not differ from the overall trend.

Until Day 9, the decline is very pronounced. By Day 11, the Oversaturated treatment has reached its lowest value before slightly recovering. By the end of the experiment, all treatments converged to similarly low values, indicating a general reduction in diatom diversity across all conditions.

The evolution of the diatom/dinoflagellate ratio over time differed significantly among treatments, as evidenced by the distinct slopes of the trend lines derived from the GLM (Fig. 6, Table 4, Table 2 Supplementary). The data are presented as Log_{10}(diatoms/dinoflagellates), which allows for a clearer visualization of relative changes in the ratio. It can be observed that C and OS treatments display similar slopes (Table 1 Supplementary), suggesting comparable trajectories in the diatom/dinoflagellate ratio over time. These slopes are steeper than those observed in other treatments, indicating more pronounced changes in the control or under oversaturated conditions. Conversely, the L, M, and H treatments, representing increasing levels of pH_{eq}OA intervention, exhibited significantly shallower slopes, indicating more gradual changes in the diatom/dinoflagellate ratio over time.

3.3. Correlations between biological and environmental variables

To further understand the drivers behind the observed changes in the diatom/dinoflagellate ratio, statistical analyses were performed to examine correlations between the log-transformed ratio and key environmental parameters. Two significant relationships emerged: 1) positive correlation with conductivity: higher conductivity values were associated with an increase in the diatom/dinoflagellate ratio. 2) Negative correlation with alkalinity: higher levels of alkalinity were linked to a decrease in the diatom/dinoflagellate ratio (Table 3 Supplementary). It is evident that the diatom/dinoflagellate ratio remains relatively stable over time in L, M, and H treatments, whereas it fluctuates markedly in both C and OS. Furthermore, higher and more stable diatom/dinoflagellate ratios are associated with higher conductivity values, as indicated by the color gradient (Fig. 7).

4. Discussion

The seawater collected in the La Spezia harbour represents a highly specific environment characterized by confined and shallow coastal conditions with strong land and anthropogenic influences (Rossi et al., 2021). These unique characteristics inherently limit the presence of planktonic calcifying organisms, such as coccolithophores, which are typically associated with open water ecosystems and display reduced diversity in coastal regions (Baumann et al., 2005). Diatoms and dinoflagellates are the predominant phytoplankton groups globally and serve as key prey for zooplankton. Diatom mineralization is not directly involved in the carbon cycle; however, diatoms significantly influence it at the global scale by biomass formation, organic C sequestration, sinking and sedimentation (Armbrust, 2009).

The starting conditions of the experiment revealed considerable heterogeneity in the diatom/dinoflagellate ratio across treatments, highlighting natural variability within the planktonic community. The log-transformed diatom/dinoflagellate ratio allowed for a more precise assessment of relative changes over time and revealed trends in dynamics that would otherwise have remained obscured. After the first seven days of the mesocosm experiment, TSi depletion marked a shift in environmental conditions that significantly impacted the dynamics of planktonic groups. Diatoms and dinoflagellates act as functional equivalents, competing for newly available nutrients, however, differences in their life cycle timing, biochemical composition, and nutritional quality, imply that variations in the diatom/dinoflagellate ratio can have far-reaching effects on the transfer of energy and matter within the ecosystem, influencing higher trophic levels (Wasmund et al., 2017). Diatoms are estimated to contribute to about 25 % of primary production on Earth (Treguer et al., 1995; Falkowski and Raven, 1997; Granum et al., 2005). They usually initiate the seasonal phytoplankton succession and form blooms until they become nutrient-limited, and other taxa with alternative nutrient acquisition strategies take over (Sommer et al., 2012). The BSi of diatom frustules is produced after uptaking of silicic acid $Si(OH)_4$ (Hildebrand and Lerch, 2015; Kristiansen and Hoel, 2002). Among the forms of DSi, $Si(OH)_4$ is often the nutrient that constrains diatom proliferation because it is highly deficient throughout most subsurface water masses upwelling into the euphotic zone (Sarmiento et al., 2004).

It is established that ocean acidification directly influences the rate of silicification in diatoms (Petrou et al., 2019; Gao and Campbell, 2014), moreover, it is well known that the response to ocean alkalinization is not perfectly opposite to that of ocean acidification (Bach et al., 2013;

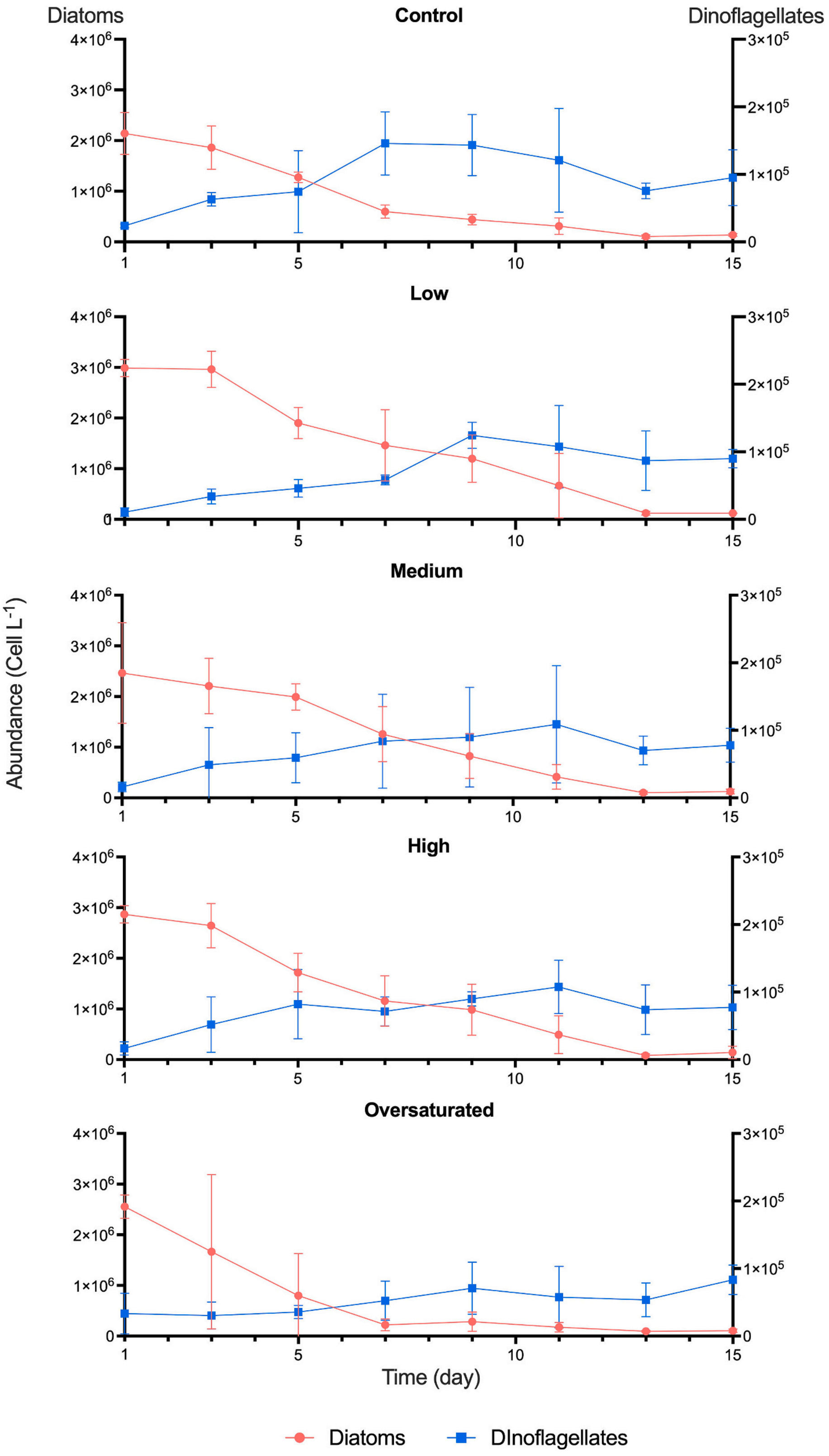

Fig. 4. Temporal variation in cell abundance (cells L^{-1}) of diatoms (orange, left scale) and dinoflagellates (blue, right scale) under different treatments. Bars for standard deviation. (For interpretation of the references to color in this figure legend, the reader is referred to the web version of this article.)

Zickfeld et al., 2021). Ferderer et al. (Ferderer et al., 2024) observed increased silicification due to the rise in total alkalinity during the initial phase of their experiment. Their findings also suggest that the response may be genus-specific, highlighting the need for further studies. Our measurements, although limited, provide support for the hypothesis that increased alkalinity may enhance silicon uptake. Uptake levels increased from C to H, with a subsequent decline observed in OS, which is likely attributable to precipitation processes.

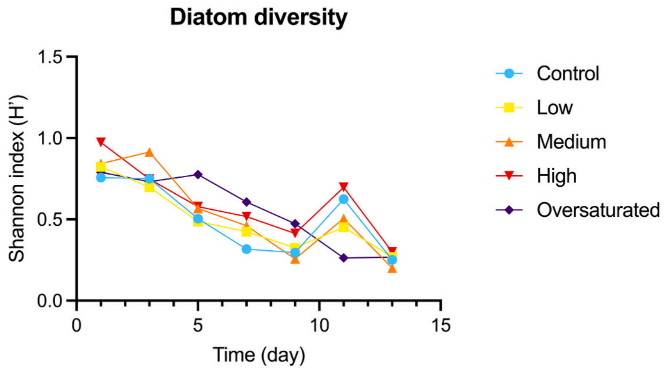

Fig. 5. Temporal variation of diatoms Shannon diversity index (H′) over 15 days under the different treatments.

Table 2
Generalised Linear Model testing treatments over time.

Tests of Between-Subjects Effects

Dependent Variable: Shannon H′

Source	SS	df	MS	F	P-value
Corrected Model	2.665[a]	5	0.533	34.807	<0.001
Intercept	15.360	1	15.360	1,003.037	<0.001
day	2.428	1	2.428	158.548	<0.001
treatn	0.237	4	0.059	3.872	0.007
Error	1.057	69	0.015		
Total	30.818	75			
Corrected Total	3.722	74			

[a] . R Squared = 0.716 (Adjusted R Squared = 0.696)

Table 3
Generalised Linear Model parameters estimates.

Parameter Estimates

Dependent Variable: Shannon H′

Parameter	B	Std. Error	t	Sig.	95 % Confidence Interval	
					Lower Bound	Upper Bound
Intercept	0.993	0.041	24.382	<0.001	0.912	1.074
day	−0.064	0.005	−12.592	<0.001	−0.074	−0.054
[treatn=C]	−0.150	0.045	−3.324	0.001	−0.240	−0.060
[treatn = L]	−0.124	0.045	−2.738	0.008	−0.214	−0.034
[treatn = M]	−0.067	0.045	−1.474	0.145	−0.157	0.024
[treatn = H]	−0.029	0.045	−0.649	0.519	−0.119	0.061
[treatn = OS]	0[a]	.	.	.	.	.

[a] . This parameter is set to zero because it is redundant.

The significantly lower slope of diatom/dinoflagellate ratio observed in the L, M, and H treatments compared to C and OS treatments suggests that pH_{eq}OA reduces the magnitude of shifts in the ratio across treatments. The effect is probably due to the higher concentration of bicarbonate in the treatments which might be uptaken by many phytoplankton organisms as the main source of inorganic carbon for photosynthesis (Nimer et al., 1997). It is believed that species able to use bicarbonate may have a competitive advantage over species using exclusively CO_2, when other essential nutrients or light are not rate-limiting for growth. Diatoms are highly efficient at utilizing HCO_3^- and typically dominate the phytoplankton community until limited by DSi. Silicon uptake rates by diatoms over a 5-day period increased with treatment intensity, from C to the high-treatment groups. C exhibited the lowest uptake, while L, M, and H treatments showed progressively higher rates, with the highest uptake observed under H and OS conditions. Overall, the data indicate a positive correlation between treatment intensity and silicon uptake (Fig. 8, Table 7 Supplementary).

The higher DSi uptake rates observed in the treatment mesocosms compared to the control may indicate that diatoms were exploiting bicarbonate resources more effectively than those in the control. Dinoflagellates also utilize bicarbonate and they may likely photosynthesize effectively at lower CO_2:HCO_3^- ratios compared to diatoms (Nimer et al., 1997). This appears consistent with the dinoflagellates increase that was observed in the mesocosms and is also supported by the negative correlation of the diatom/dinoflagellate ratio with alkalinity, which implies that increased buffering capacity may favour dinoflagellates, possibly by modulating carbonate chemistry in a way that benefits their cellular processes. The stabilization effect observed in the L, M, and H treatments could enhance ecological resilience by maintaining a more balanced community structure under changing conditions. Heterogeneity at the initial time point, indicative of natural system variability, likely influenced community responsiveness to treatments. While alkalinity serves as a marker of treatment intensity, the primary co-benefit appears to be the increased availability of bicarbonate, which could directly support phytoplankton growth. Diatoms, in particular, are known to actively take up HCO_3^- through carbon-concentrating mechanisms involving SLC-4 transporters and carbonic anhydrase activity, enabling efficient carbon acquisition under variable carbonate chemistry (Tortell et al., 1997; Matsuda et al., 2017). Salinity, on the other hand, affects an organism's ability to maintain ion homeostasis, increasing the energetic demand required to regulate osmotic balance and ionic gradients (Volkov, 2015). The observed correlation between salinity (conductivity) and the diatom/dinoflagellate ratio, in turn, significantly influences community composition, suggesting that species-specific responses to both carbonate availability and ionic regulation play a key role in determining differences among the phytoplankton components (Elferink et al., 2020). This distinction underscores the complex interplay between carbonate system dynamics, ion regulation, and phytoplankton community structure in response to ocean alkalinization. The observed decline in diatom diversity across all treatments suggests a strong impact of experimental conditions on community structure and it is likely due to environmental stressors introduced by the depletion of DSi. Diatoms require DSi for the formation of their frustules, and a reduction in its availability can lead to competitive disadvantages and to a consequent loss of diversity (Petrou et al., 2019).

An important consideration is the potential for this process to favour silicifying organisms, which could, in turn, lead to a net increase in CO_2 sequestration in the deep ocean (Bach et al., 2019). $CaCO_3$ has higher density (2.7 g cm^{-3}) compared to biogenic silica (BSi, amorphous SiO_2, 2.1 g cm^{-3}) and is generally considered more effective at accelerating the sinking of organic matter into the deep ocean (Klaas and Archer, 2002). $CaCO_3$ ballast is currently regarded as significant only in specific regions, while the influence of BSi ballast is thought to be more widespread across the oceans (Wilson et al., 2012; Le Moigne et al., 2014; Tréguer et al., 2018). An increase in diatom biomass could enhance the ballast potential of BSi. This, in turn, may amplify carbon export in silicate-based enhanced weathering (EW) and ocean alkalinity enhancement (OAE) schemes (Köhler et al., 2013). Diatoms were the dominant component of the phytoplankton community in La Spezia harbour waters, consistently with studies on similar environments. Carbonate-producing plankton are generally rare in these conditions, making significant CO_2 release from calcification unlikely. Our results also support evidence that higher alkalinity may increase silicon uptake. While the study provides valuable insights, certain limitations should be acknowledged. The initial large variability in the system may hamper the possibility of a straightforward export of our results to different environmental settings. Future research could expand on these findings by incorporating additional environmental parameters, and a suite of

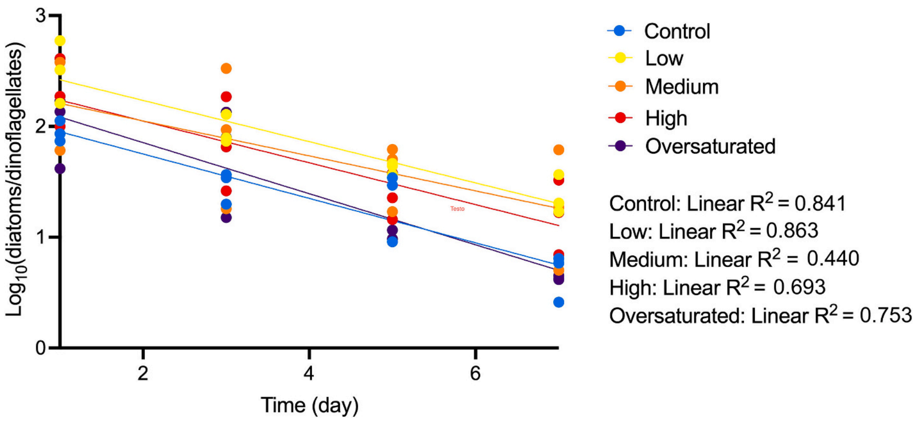

Fig. 6. Temporal variation of the log-transformed diatom/dinoflagellate ratio over 7 days under different treatment.

Table 4
Test of effects between subjects. The ANOVA table evaluates the effect of time and treatment on the log-transformed diatom/dinoflagellate ratio.

Dependent variable: log diatom dinoflagellates

Origin	Sum of type III squares	df	Quadratic mean	F	P-value
Correct model	9,032[a]	4	2,258	28,262	<0.001
Intercept	64,716	1	64,716	809,961	<0.001
Time (days)	7,487	1	7,487	93,699	<0.001
Treatment	1,546	3	,515	6,449	,001
Error	3,436	43	,080		
Total	146,842	48			
Total corrected	12,468	47			

[a] . R-square =,724 (adjusted R-square =,699)

diverse geographic contexts to improve the understanding of plankton dynamics under pH$_{eq}$OA.

5. Conclusions

Our results provide a pioneering glimpse into the efficacy and potential ecological effects of pH-equilibrated ocean alkalinization (pH$_{eq}$OA) using Limenet® technology in harbour water. The observed effects of pH$_{eq}$OA interventions on phytoplankton communities indicate that these treatments may moderate the rate of change in the diatom/dinoflagellate ratio, thereby enhancing ecological stability in sensitive aquatic ecosystems. In the Control treatment, this rate of change is assumed to result from mesocosm effects and associated environmental conditions, whereas in the Oversaturated treatment it is likely driven by carbonate precipitation The differing effects of conductivity and alkalinity highlight the importance of considering specific abiotic factors in management strategies. Our results also provide further evidence that higher alkalinity may increase silicon uptake. Since diatoms play a major role in carbon sequestration, these findings indicate that the technology provides an added benefit by boosting their growth. Further research should include more environmental factors and varied geographic settings to better understand plankton dynamics under pH$_{eq}$OA.

Glossary

AWL	Accelerated Weathering of Limestone
BAWL	Buffered Accelerated Weathering of Limestone
BSi	Biogenic (amorphous) Silica, SiO_2

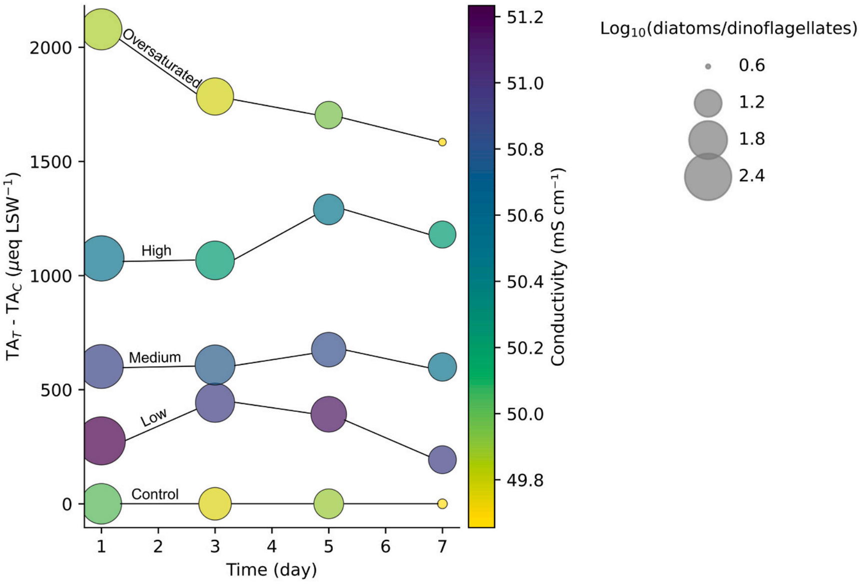

Fig. 7. Correlation between alkalinity, conductivity and Log$_{10}$(diatoms/dinoflagellates) across time and under different treatment conditions (Control, Low, Medium, High, and Oversaturated). Bubble size is the Log$_{10}$(diatoms/dinoflagellates), bubble color indicates conductivity (mS cm^{-1}).

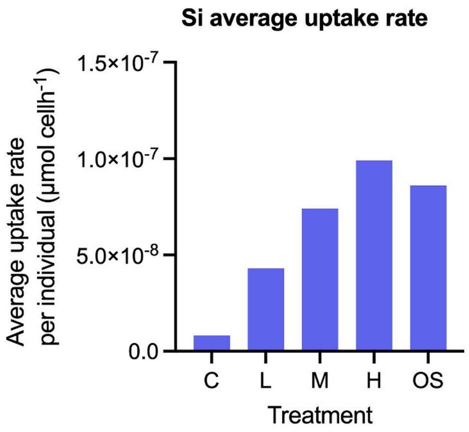

Fig. 8. Si uptake across treatment, estimated from diatom abundances of day 1.

CCMs	CO_2 Concentrating Mechanisms
CDR	Carbon Dioxide Removal
DIC	Dissolved Inorganic Carbon
DSi	Dissolved Silica, mostly $Si(OH)_4$
DO	Dissolved Oxygen
GLM	Generalised Linear Model
HABs	Harmful Algal Blooms
LCA	Life Cycle Assessment
LDPE	Low-Density PolyEthylene
NET	Negative Emissions Technology
OAE	Ocean Alkalinity Enhancement
$pH_{eq}OA$	pH-equilibrated Ocean Alkalinization
TA	Total Alkalinity
TA_C	Total Alkalinity Control
TA_T	Total Alkalinity Treatment
TSi	Total Silicon
TRL	Technology Readiness level
Ω_{arag}	Aragonite saturation state

CRediT authorship contribution statement

Sara Groppelli: Writing – review & editing, Writing – original draft, Methodology, Investigation, Data curation, Conceptualization. **Davide Calvi:** Methodology, Investigation, Conceptualization. **Federico Comazzi:** Writing – review & editing, Investigation. **Samira Jamali Alamooti:** Writing – review & editing, Investigation. **Arianna Azzellino:** Writing – review & editing, Formal analysis, Data curation. **Eleonora Barbaccia:** Writing – review & editing, Formal analysis, Data curation. **Sarah Caronni:** Resources, Formal analysis. **Piero Macchi:** Writing – review & editing, Validation, Supervision, Resources. **Guido Raos:** Writing – review & editing, Validation, Resources. **Daniela Basso:** Writing – review & editing, Validation, Supervision, Resources, Methodology, Conceptualization.

Funding sources

The temporary facility that hosted the experiment and the logistics were funded by Limenet s.r.l. SG and DC were supported by a PNRR PhD fellowship of the Milano-Bicocca University (code 39>–033-C6-DOT13C6527–9463 and 39–033-C6-DOT13C6527–9024, respectively). SJA was supported by a PNRR PhD fellowship of Politecnico di Milano (39–033-16-DOT1316197–9926).

Declaration of competing interest

The authors declare the following financial interests/personal relationships which may be considered as potential competing interests: Sara Groppelli reports financial support was provided by Limenet s.r.l. Federico Comazzi reports a relationship with Limenet s.r.l. that includes: employment. Sara Groppelli reports a relationship with Limenet s.r.l. that includes: travel reimbursement. Davide Calvi reports a relationship with Limenet s.r.l. that includes: travel reimbursement. The PhD fellowship of SG, DC and SJ have been partially funded by Limenet under the scientific independent supervision of the University of Milano-Bicocca (SG and DC) and Politecnico di Milano (SJA) respectively. If there are other authors, they declare that they have no known competing financial interests or personal relationships that could have appeared to influence the work reported in this paper. If there are other authors, they declare that they have no known competing financial interests or personal relationships that could have appeared to influence the work reported in this paper.

Acknowledgements

We would like to express our gratitude to Valeria Mezzanotte, Emilio Brivio Sforza, and Maria Tringali for their invaluable contribution to the analysis of dissolved inorganic nutrients. We also thank Francesco Campo for his support in the organisation and management of the project. Our sincere appreciation goes to Sandra Citterio for providing the necessary instruments for the phytoplankton analysis. We extend our thanks to Porto di Mirabello for providing the location and allowing the execution of the experiment, with special gratitude to Claudia Guerra and Barbara Martinelli for their valuable support. Furthermore, we would like to express our gratitude to Pierluigi Peracchini, Mayor of La Spezia, Mario Sommariva, President of the Port Authority, and Dr. Giovanna Visco from the Port Authority for their valuable support. We also sincerely thank Dr. Stefano Molino, Senior Partner, Head of Accelerator Fund at CDP Venture Capital, for his contribution. DB, AA, PM are grateful to the OACIS project n. 4000.1-1 of the Fondation Prince Albert II de Monaco for creating the broader scientific context in which this experiment was conceived.

Appendix A. Supplementary data

Supplementary data to this article can be found online at https://doi.org/10.1016/j.marpolbul.2025.118787.

Data availability

Data will be made available on request.

References

Alexander, A.C., Luiker, E., Finley, M., Culp, J.M., 2016. Mesocosm and Field Toxicity Testing in the Marine Context. In: *Marine Ecotoxicology:* Current Knowledge and Future Issues. https://doi.org/10.1016/B978-0-12-803371-5.00008-4.

Armbrust, E. V. (2009). The life of diatoms in the world's oceans. In *Nature* (Vol. 459, issue 7244). doi:https://doi.org/10.1038/nature08057.

Avancini, M., Cicero, A.M., Di Girolamo, I., Innamorati, M., Magaletti, E., 2006. In: Sertorio Zunini, T. (Ed.), Guida al riconoscimento del plancton dei mari italiani, Vol. I – Fitoplancton. Ministero dell'Ambiente e della Tutela del Territorio e del Mare – ICRAM, Roma eds.

Bach, L.T., MacKinder, L.C.M., Schulz, K.G., Wheeler, G., Schroeder, D.C., Brownlee, C., Riebesell, U., 2013. Dissecting the impact of CO2 and pH on the mechanisms of photosynthesis and calcification in the coccolithophore Emiliania huxleyi. New Phytol. 199 (1). https://doi.org/10.1111/nph.12225.

Bach, Lennart Thomas, Hernández-Hernández, Nauzet, Taucher, Jan, Spisla, Carsten, Sforna, Claudia, Riebesell, Ulf, Arístegui, Javier, 2019. Effects of elevated CO2 on a natural diatom community in the subtropical North East Atlantic [dataset publication series]. PANGAEA, doi:10.1594/PANGAEA.898596, Supplement to: Bach, LT et al. (2019): Effects of elevated CO2 on a natural diatom Community in the Subtropical NE Atlantic. Front. Mar. Sci 6. https://doi.org/10.3389/fmars.2019.00075.

Baumann, K.-H., Andruleit, H., Böckel, B., Geisen, M., Kinkel, H., 2005. The significance of extant coccolithophores as indicators of ocean water masses, surface water temperature, and palaeoproductivity: a review. Paläontol. Z. 79 (1). https://doi.org/10.1007/bf03021756.

Calbet, A., 2008. The trophic roles of microzooplankton in marine systems. ICES J. Mar. Sci. 65 (3). https://doi.org/10.1093/icesjms/fsn013.

Caldeira, K., Rau, G.H., 2000. Accelerating carbonate dissolution to sequester carbon dioxide in the ocean: geochemical implications. Geophys. Res. Lett. 27, 225–228.

Camatti, E., Valsecchi, S., Caserini, S., Barbaccia, E., Santinelli, C., Basso, D., Azzellino, A., 2024. Short-term impact assessment of ocean liming: a copepod exposure test. Mar. Pollut. Bull. 198. https://doi.org/10.1016/j.marpolbul.2023.115833.

Caserini, S., Cappello, G., Righi, D., Raos, G., Campo, F., De Marco, S., Renforth, P., Varliero, S., Grosso, M., 2021. Buffered accelerated weathering of limestone for storing CO2: chemical background. International Journal of Greenhouse Gas Control 112. https://doi.org/10.1016/j.ijggc.2021.103517.

Cicero, A.M., Di Girolamo, I., 2001. Metodologie analitiche di riferimento del programma di monitoraggio per il controllo dell'ambiente marino costiero (triennio 2001–2003). Ministero dell'Ambiente e della Tutela del Territorio, ICRAM, Roma.

Ciuffardi, T., Giuliani, A., Barsanti, M., Bordone, A., Cerrati, G., Di Nallo, G., Picco, P., 2013. Quarant'anni di dati oceanografici a cura del centro ricerche ambiente marino ENEA s. Teresa: il quadro del golfo di La Spezia. In: *Distribuzione Storica Dei Dati Dal* 1973 Al 2013. ENEA, TR 2013–09, pp. 18–24.

De Marco, S., Varliero, S., Caserini, S., Cappello, G., Raos, G., Campo, F., Grosso, M., 2023. Techno-economic evaluation of buffered accelerated weathering of limestone as a CO2 capture and storage option. Mitig. Adapt. Strateg. Glob. Change 28, 17.

Dickson, A.G., 1990. Thermodynamics of the dissociation of boric acid in synthetic seawater from 273.15 to 318.15K. Deep-Sea Res. 37, 755–766.

Dickson, A.G., Millero, F.J., 1987. A comparison of the equilibrium constants for the dissociation of carbonic acid in seawater media. Deep-Sea Res. 34, 1733–1743.

Elferink, S., John, U., Neuhaus, S., Wohlrab, S., 2020. Functional Genomics Differentiate Inherent and Environmentally Influenced Traits in Dinoflagellate and Diatom Communities. Microorganisms Apr 15;8 (4), 567. https://doi.org/10.3390/microorganisms8040567. PMID: 32326461; PMCID: PMC7232425.

Exley, C., Sjöberg, S., 2014. Silicon species in seawater. Spectrochim. Acta A Mol. Biomol. Spectrosc. 117, 820–821. https://doi.org/10.1016/j.saa.2013.09.002.

Falkowski, P.G., Raven, J.A., 1997. Aquatic Photosynthesis. Blackwell Science, Oxford, UK.

Ferderer, A., Schulz, K.G., Riebesell, U., Baker, K.G., Chase, Z., Bach, L.T., 2024. Investigating the effect of silicate- and calcium-based ocean alkalinity enhancement on diatom silicification. Biogeosciences 21, 2777–2794. https://doi.org/10.5194/bg-21-2777-2024.

Foteinis, S., Andresen, J., Campo, F., Caserini, S., Renforth, P., 2022. Life cycle assessment of ocean liming for carbon dioxide removal from the atmosphere. J. Clean. Prod. 370. https://doi.org/10.1016/j.jclepro.2022.133309.

Fuss, S., Lamb, W.F., Callaghan, M.W., Hilaire, J., Creutzig, F., Amann, T., Beringer, T., De Oliveira Garcia, W., Hartmann, J., Khanna, T., Luderer, G., Nemet, G.F., Rogelj, J., Smith, P., Vicente, J.V., Wilcox, J., Del Mar Zamora Dominguez, M., Minx, J.C., 2018. Negative emissions - part 2: costs, potentials and side effects. Environ. Res. Lett. 13 (6). https://doi.org/10.1088/1748-9326/aabf9f.

Gao, K., Campbell, D.A., 2014 Apr. (2014). Photophysiological responses of marine diatoms to elevated CO2 and decreased pH: a review. Funct. Plant Biol. 41 (5), 449–459. https://doi.org/10.1071/FP13247. 32481004.

Granum, E., Raven, J.A., Leegoog, R.C., 2005. How do marine diatoms fix 10 billion tonnes of inorganic carbon per year? Can. J. Bot. 83, 898–908.

Hildebrand, M., Lerch, S.J., 2015. Diatom silica biomineralization: parallel development of approaches and understanding. Semin. Cell Dev. Biol. 2015 Oct;46, 27–35. https://doi.org/10.1016/j.semcdb.2015.06.007. Epub 2015 Aug 7. PMID: 26256954.

Hopkinson, B.M., 2014. A chloroplast pump model for the CO2 concentrating mechanism in the diatom Phaeodactylum tricornutum. Photosynth. Res. 121 (2–3). https://doi.org/10.1007/s11120-013-9954-7.

Iglesias-Rodríguez, M.D., Rickaby, R.E.M., Singh, A., Gately, J.A., 2023. Laboratory experiments in ocean alkalinity enhancement research. State Planet. Discuss. 2023 (July).

Intergovernmental Panel on Climate Change (IPCC), 2022. Climate Change 2022—Mitigation of Climate Change: Working Group III Contribution to the Sixth Assessment Report of the Intergovernmental Panel on Climate Change. Cambridge University Press, Cambridge, UK.

IPCC, 2014. In: Edenhofer, O. (Ed.), Climate Change 2014: Mitigation of Climate Change Contribution of Working Group III to the Fifth Assessment Report of the Intergovernmental Panel on Climate Change Ed. Cambridge: Cambridge University Press.

Klaas, C., Archer, D.E., 2002. Association of sinking organic matter with various types of mineral ballast in the deep sea: implications for the rain ratio. Glob. Biogeochem. Cycles 16, 1–14. https://doi.org/10.1029/2001GB001765.

Köhler, P., Abrams, J.F., Völker, C., Hauck, J., Wolf-Gladrow, D.A., 2013. Geoengineering impact of open ocean dissolution of olivine on atmospheric CO2, surface ocean pH and marine biology. Environ. Res. Lett. 8, 014009. https://doi.org/10.1088/1748-9326/8/1/014009.

Kristiansen, S., Hoel, E.E., 2002. The importance of silicon for marine production. Hydrobiologia 484, 21–31, 2002.

Kristiansen, S., Hoell, E.E., 2002. The importance of silicon for marine production*. Hydrobiologia 484, 21–31. https://doi.org/10.1023/A:1021392618824.

Kruger, T., Renforth, P., 2012, April. Engineering challenges of ocean alkalinity enhancement. In: In *EGU general assembly conference abstracts*, p. 8513 p.

Le Moigne, F.A.C., Pabortsava, K., Marcinko, C.L.J., Martin, P., Sanders, R.J., 2014. Where is mineral ballast important for surface export of particulate organic carbon in the ocean? Geophys. Res. Lett. 41, 1–9. https://doi.org/10.1002/2014GL061678.

Limenet®, 2024. United States Patent and Trademark—Office. Apparatus and Method for Accelerated Dissolution of Carbonates with Buffered. In: European Patent. PHPCT/IB2022/051464. *WO2022175885*, 29 July 2024.

Marañón, E., 2015. Cell size as a key determinant of phytoplankton metabolism and community structure. Ann. Rev. Mar. Sci. 7. https://doi.org/10.1146/annurev-marine-010814-015955.

Matsuda, Y., Hopkinson, B.M., Nakajima, K., Dupont, C.L., Tsuji, Y., 2017. Mechanisms of carbon dioxide acquisition and CO_2 sensing in marine diatoms: a gateway to carbon metabolism. Philos. Trans. R. Soc., B 372 (1720), 20160403. https://doi.org/10.1098/rstb.2016.0403.

Mayot N., Nival P., Lévy M. (2020). Primary production in the Ligurian Sea. Christophe Migon; Paul Nival; Antoine Sciandra. The Mediterranean Sea in the era of global change 1: 30 years of multidisciplinary study of the Ligurian Sea, 1, Wiley, pp.139-164, 2020, 9781786304285. ⟨https://doi.org/10.1002/9781119706960.ch6⟩. ⟨hal-03003497⟩.

Mehrbach, C., Culberson, C.H., Hawley, J.E., Pytkowicx, R.M., 1973. Measurement of the apparent dissociation constants of carbonic acid in seawater at atmospheric pressure. Limnol. Oceanogr. 18. https://doi.org/10.4319/lo.1973.18.6.0897.

Moras, C.A., Bach, L.T., Cyronak, T., Joannes-Boyau, R., Schulz, K.G., 2022. Ocean alkalinity enhancement – avoiding runaway $CaCO_3$ precipitation during quick and hydrated lime dissolution. Biogeosciences 19, 3537–3557. https://doi.org/10.5194/bg-19-3537-2022.

Moreno, H.D., Köring, M., Di Pane, J., Tremblay, N., Wiltshire, K.H., Boersma, M., Meunier, C.L., 2022. An integrated multiple driver mesocosm experiment reveals the effect of global change on planktonic food web structure. Communications Biology 5 (1). https://doi.org/10.1038/s42003-022-03105-5.

National Academies of Sciences, Engineering, and Medicine, 2019. Negative Emissions Technologies and Reliable Sequestration: A Research Agenda. The National Academies Press, Washington, DC. https://doi.org/10.17226/25259.

Nimer, N.A., Iglesias-Rodriguez, M.D., Merrett, M.J., 1997. BICARBONATE UTILIZATION BY MARINE PHYTOPLANKTON SPECIES. J. Phycol. 33, 625–631. https://doi.org/10.1111/j.0022-3646.1997.00625.x.

Pedersen, M.F., Hansen, P.J., 2003. Effects of high pH on the growth and survival of six marine heterotrophic protists. Mar. Ecol. Prog. Ser. 260. https://doi.org/10.3354/meps260033.

Petrou, K., Baker, K.G., Nielsen, D.A., et al., 2019. Acidification diminishes diatom silica production in the Southern Ocean. Nat. Clim. Chang. 9, 781–786. https://doi.org/10.1038/s41558-019-0557-y.

Pierrot, D., Lewis, E., Wallace, D., 2006. MS excel program developed for CO2 system calculations. In: Carbon Dioxide Information Analysis Center, oak Ridge National Laboratory, U.S. Department of Energy. Oak Ridge, Tennessee.

Rau, G.H., Caldeira, K., 1999. Enhanced carbonate dissolution: a means of sequestering waste CO2 as ocean bicarbonate. Energ. Conver. Manage. 40, 1803–1813.

Raven, J.A., Giordano, M., Beardall, J., Maberly, S.C., 2011. Algal and aquatic plant carbon concentrating mechanisms in relation to environmental change. Photosynth. Res. 109 (1–3). https://doi.org/10.1007/s11120-011-9632-6.

Riebesell, U., Basso, D., Geilert, S., Dale, A.W., Kreuzburg, M., Oschlies, A., Stevenson, A., Bach, L.T., Fennel, K., Rickaby, R.E.M., Satterfield, T., Webb, R., Gattuso, J.-P., 2023. Mesocosm experiments in ocean alkalinity enhancement research, in: Guide to Best Practices in Ocean Alkalinity Enhancement Research, edited by. Copernicus Publications, State Planet 6. https://doi.org/10.5194/sp-2-oae2023-6-2023, 2-oae2023.

Rogelj, J., Shindell, D., Jiang, K., Fifita, S., Forster, P., Ginzburg, V., Handa, C., Kheshgi, H., Kobayashi, S., Kriegler, E., Mundaca, L., Séférian, R., Vilariño, M.V., 2018. Mitigation pathways compatible with 1.5°C in the context of sustainable development. In: global warming of 1.5°C. In: IPCC special report global warming of 1.5 °C.

Rossi, V., Amorosi, A., Marchesini, M., Marvelli, S., Cocchianella, A., Lorenzini, L., Trigona, S.L., Valle, G., Bini, M., 2021. Late quaternary landscape dynamics at the La Spezia gulf (NW Italy): a multi-proxy approach reveals environmental variability within a rocky embayment. Water 13, 427. https://doi.org/10.3390/w13040427.

Rutherford, A., 2001. Introducing Anova and Ancova: A GLM Approach (Introducing Statistical Methods Series). SAGE Publications.

Sánchez N, Goldenberg SU, Brüggemann D, Jaspers C, Taucher J, Riebesell U. (2024). Plankton food web structure and productivity under ocean alkalinity enhancement. Sci Adv. 2024 Dec 6;10(49):eado0264. doi:https://doi.org/10.1126/sciadv.ado0264. Epub 2024 Dec 6. PMID: 39642213; PMCID: PMC11623272.

Sarmiento, J.L., Gruber, N., Brzezinski, M.A., Dunne, J.P., 2004. High-latitude controls of thermocline nutrients and low latitude biological productivity. Nature 427, 56–60. https://doi.org/10.1038/nature 02127.

Shannon, C.E., 1948. A mathematical theory of communication. The Bell Syst. Tech. J. 27, 379–423.

Sommer, U., Adrian, R., De Senerpont Domis, L., Elser, J.J., Gaedke, U., Ibelings, B., et al., 2012. Beyond the plankton ecology group (PEG) model: mechanisms driving plankton succession. Annu. Rev. Ecol. Evol. Syst. 43, 429–448. https://doi.org/10.1146/annurev-ecolsys-110411-1 60251.

Spreitzer, R.J., Salvucci, M.E., 2002. Rubisco: structure, regulatory interactions, and possibilities for a better enzyme. In. Annu. Rev. Plant Biol. 53. https://doi.org/10.1146/annurev.arplant.53.100301.135233.

Suitner, N., Faucher, G., Lim, C., Schneider, J., Moras, C.A., Riebesell, U., Hartmann, J., 2024. Ocean alkalinity enhancement approaches and the predictability of runaway precipitation processes: results of an experimental study to determine critical alkalinity ranges for safe and sustainable application scenarios. Biogeosciences 21, 4587–4604. https://doi.org/10.5194/bg-21-4587-2024.

Terlouw, T., Bauer, C., Rosa, L., Mazzotti, M., 2021. Life cycle assessment of carbon dioxide removal technologies: a critical review. Energ. Environ. Sci. 14, 1701–1721. https://doi.org/10.1039/d0ee03757e.

Tortell, P., Reinfelder, J., Morel, F., 1997. Active uptake of bicarbonate by diatoms. Nature 390, 243–244. https://doi.org/10.1038/36765.

Traboni, C., Nocera, A., Romano, F., Courboulès, J., Chantzaras, C., Magiopoulos, I., Varliero, S., Basso, D., & Pitta, P. (in press) Plankton don't care: minimal effects of ocean liming on plankton growth and grazing in the eastern Mediterranean. Limnol. Oceanogr.

Tréguer, P., Bowler, C., Moriceau, B., Dutkiewicz, S., Gehlen, M., Aumont, O., et al., 2018. Influence of diatomdiversity on the ocean biological carbon pump. Nat. Geosci. 11, 27–37. https://doi.org/10.1038/s41561-017-0028-x.

Treguer, P., Nelson, D.M., Bennekom, A.J., Demaster, D.J., Leynaert, A., Queguiner, B., 1995. The silica balance in the world ocean: a re-estimate. Science 268, 375–379.

Uppström, L.R., 1974. The boron/chlorinity ratio of deep-sea water from the Pacific Ocean. Deep-Sea Res. I 21, 161–162.

Varliero, S., Jamali Alamooti, S., Campo, F.P., Cappello, G., Cappello, S., Caserini, S., Raos, G., 2024. Assessing the limit of CO2 storage in seawater as bicarbonate-enriched solutions. Molecules 29 (17), 4069.

Volkov, V., 2015. Salinity tolerance in plants. Quantitative approach to ion transport starting from halophytes and stepping to genetic and protein engineering for manipulating ion fluxes. Front. Plant Sci. Oct 27;6, 873. https://doi.org/10.3389/fpls.2015.00873 (PMID: 26579140; PMCID: PMC4621421).

Wasmund, N., Kownacka, J., Göbel, J., Jaanus, A., Johansen, M., Jurgensone, I., Lehtinen, S., Powilleit, M., 2017. The diatom/dinoflagellate index as an indicator of ecosystem changes in the Baltic Sea 1. principle and handling instruction. Front. Mar. Sci. 4 (FEB). https://doi.org/10.3389/FMARS.2017.00022.

Wilson, J.D., Barker, S., Ridgwell, A., 2012. Assessment of the spatial variability in particulate organic matter and mineral sinking fluxes in the ocean interior: implications for the ballast hypothesis. Global Biogeochem. Cycles 26, GB4011. https://doi.org/10.1029/2012GB004398.

Xin, X., Goldenberg, S.U., Taucher, J., Stuhr, A., Arístegui, J., Riebesell, U., 2024. Resilience of phytoplankton and microzooplankton communities under ocean alkalinity enhancement in the Oligotrophic Ocean. Environ. Sci. Technol. 58 (47), 20918–20930.

Zeebe, R. and Wolf-Gladrow, D. (2001): CO2 in Seawater: Equilibrium, Kinetics, Isotopes, Elsevier Oceanography Book Series, 65, 346 pp, Amsterdam, ISBN: 0–444–50946-1 and 0.

Zickfeld, K., Azevedo, D., Mathesius, S., Matthews, H.D., 2021. Asymmetry in the climate–carbon cycle response to positive and negative CO2 emissions. Nature Climate Change 11 (7). https://doi.org/10.1038/s41558-021-01061-2.

Zingone, A., Totti, C.M., Sarno, D., Cabrini, M., Caroppo, C., Giacobbe, M.G., Lugliè, A., Nuccio, C., Socal, G., 2010. Fitoplancton: Metodiche Di Analisi Quali-Quantitativa. In: Metodologie di Campionamento e di Studio del Plancton Marino. ISPRA, Rome, Italy, pp. 213–237. Volume 56, pp. ISBN 88-448-0427-1.